Computation of the energy distribution of localised states from transient photo-decay measurements on disordered semiconductors: a comparison of methods♣

C. MAIN[*], J. M. MARSHALL[a]
University of Dundee, Division of Electronic Engineering and Physics, Dundee DD1 4HN, U.K.
[a]*Emeritus Professor, School of Engineering, University of Wales Swansea, U.K.*

A computer simulation technique is employed to calculate the transient photo-decay characteristics for a disordered semiconductor featuring an exponential tail of localized states plus a narrow Gaussian feature of adjustable height. The resulting data are subjected to analysis via the "pre-transit" ($1/i(t).t$), "post-transit" ($i(t).t$) and "Fourier Transform" procedures. It is shown that all three options can detect the presence of the Gaussian component. However, even when the peak height of this becomes comparable to or less than that of the local exponential background, the pre-transit procedure consistently miscalculates its energy. In contrast, the post-transit and Fourier transform procedures correctly identify this energy, and also provide improved resolution of the energy distribution and other properties of the localized states. We discuss further the theory and application of the Fourier Transform procedures to the analysis of $i(t)$ data, focusing in particular on the effect of the inevitable short and long time truncation of $i(t)$ data in experimental measurements. We show how some simple measures can be taken to extend the energy range and accuracy of the method in the determination of density-of-states distributions.

1. Introduction

It has long been recognized that in the case of trap-limited band transport in disordered semiconductors, transient photo-decay measurements have the *potential* to provide information on the energy distribution, and possibly other characteristics, of the localized states involved. In particular, an exponential density-of-states (DOS) distribution yields (after the initial carrier trapping regime) a featureless power-law decay in the current, $I(t)$, with elapsed time after carrier generation, t, while the presence of additional structure in the DOS can give rise to significant deviations from this (e.g. [1,2]).

In the "pre-transit" regime of the photo-decay response (i.e. in the absence of carrier losses by arrival at an extraction electrode or by recombination), a simple procedure was proposed ([3], following the model advanced in [4]) for interpreting *suitable* experimental data. In this "pre-transit" technique (following completion of the initial free carrier trapping regime), the DOS, $g(E_{th})$ ($cm^{-3}eV^{-1}$), at energy $E_{th} = kT \ln(\nu t)$ was predicted to be

$$g(E_{th}) = (I(t=0) g(E_c) \nu^{-1})/(I(t) t). \qquad (1)$$

Here, T is the temperature, ν the "attempt to escape" frequency for trapped carriers, $I(t=0)$ the transient photocurrent at zero time (i.e. the product of the number of excess carriers per unit specimen thickness, the electronic charge, the free carrier mobility and the applied electric field), and $g(E_c)$ the density of states at the mobility edge separating extended from localized states. The rationale for the choice of E_{th} arose from the concept of a "thermalization energy", such that the release time constant for states at this depth, $\nu^{-1}\exp(E_{th}/kT)$, is equal to the elapsed time t. It was envisaged that shallower levels will have had sufficient time to achieve quasi-thermal equilibrium with the extended transport states, while deeper traps will not. For the case of a *slowly* decaying *exponential* DOS, this was predicted to yield a reasonably sharp peak in the trapped carrier density close to E_{th} [4], leading straightforwardly [3] to the above analytical procedure.

Although this procedure worked well in the case of a *purely exponential* DOS, it soon became clear that problems arose in the case of more complex energy distributions. Indeed, for a very highly structured DOS, it

---

♣ Paper presented at the International School on Condensed Matter Physics, Varna, Bulgaria, September 2008

could even yield the complete inverse of the true energy distribution (e.g. [2]).

The resulting impression was that the pre-transit procedure *should* be acceptable, provided any structure in the DOS was "not very pronounced", but would become invalid for more highly structured distributions. However, to the best of our knowledge, the definition of "not very pronounced", and indeed whether the pre-transit analysis is valid *even then*, has not been properly explored. It was one of the main objectives of the present study to make such an evaluation.

We will also examine the viability of the "post-transit" procedure ([3] and references therein), which predicts the relationship

$$g(E_{th}) = CI(t)t \qquad (2)$$

Here, C is a constant subsequently [5] quantified as 2 $g(E_c)/(Q_0 \, t_0 \, \nu)$, where Q_0 is the total charge and t_0 the *free carrier* transit time. However, since at least one of these parameters (t_0) may well not easily be estimated from experimental data, it is more common in practice to perform normalized calculations of the DOS, using such data.

A subsequent alternative [6,7] to the above analytical techniques, although admittedly less straightforward to apply, involved a Fourier transformation of the current vs. time measurements into the frequency (ω) domain, followed by an analysis of the resulting data to yield the DOS.

In its simplest form, the one-sided Digital Fourier Transform (DFT) $I(\omega_n)$, of the time-sampled signal $i(t_k)$ may be approximated by cosine and sine summations *viz*,

$$I(\omega_n) = \sum_k i(t_k) \begin{Bmatrix} \cos(\omega_n t_k) \\ -j\sin(\omega_n t_k) \end{Bmatrix} \Delta t_k = i_p - ji_q \quad (3)$$

In practice, we have employed linear spline fitting between successive points, and a piecewise- analytic integration scheme. The DOS may then be obtained, [8,9]

$$g(E_n) \approx \frac{1}{\nu \sigma kT} \omega_n \frac{d}{d\omega} \left(\frac{e\mu\varepsilon AG \cos(\phi(\omega_n))}{|I(\omega_n)|} \right), \qquad (4)$$

with the energy scale being

$$E_n = kT \ln(\nu/\omega_n), \qquad (5)$$

where ν is as in Eq. 1, σ is the capture cross-section, e the electronic charge, μ the electron mobility, ε the electric field strength, and A the conduction cross section. G is the effective ac amplitude of optical generation at frequency ω, i.e. the Fourier Transform of the impulse excitation, and ϕ is the phase lag between this ac excitation and the photocurrent.

Here, it is important to note that although the resulting energy scale $E(\omega_n)$, may *appear* equivalent to that for the thermalization energy, E_{th}, the analysis carries no

implication of, or indeed requirement for, a peak in the occupied state density close to this energy. Rather, the procedure employs the *full* available time range of the experimental data in performing the transform for any particular value of ω and hence $E(\omega)$.

2. The computer simulation procedure and results for the "pre-transit" case

The model DOS employed in this study, as shown in Fig. 1, featured an exponential bandtail of the form $g_e(E) = g(E_c) \exp(-E/kT_o)$, with $g(E_c) = 4 \times 10^{21}$ cm^{-3}eV^{-1} and with $T_o = 600$ K as the characteristic temperature for the exponential component. To this was added a relatively narrow Gaussian component of the form $g(E_{pk}) \exp(-0.5((E-E_{pk})/E_w)^2))$, where $E_{pk} = 0.35$ eV was the peak energy of the feature and $E_w = 0.025$ eV its width parameter. The peak height, $g(E_{pk})$, was varied via a multiplying factor, M, with respect to the value of the background exponential component at a depth of 0.35 eV, i.e. $g(E_{pk}) = M \times g(E_c) \exp(-0.35/kT_o) = 4.5 \times 10^{18}$ M cm^{-3}eV^{-1} for the above parameters.
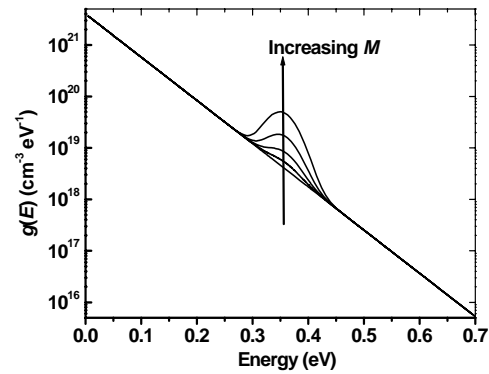
Fig. 1. DOS employed in the simulation study, as described in the text.

Fig. 2 shows the resulting transient photocurrents, as computed at a measurement temperature of 300 K, using the technique outlined in [10], in the "pre-transit" regime (i.e. with no carrier losses due to arrival at an extraction electrode or to recombination).
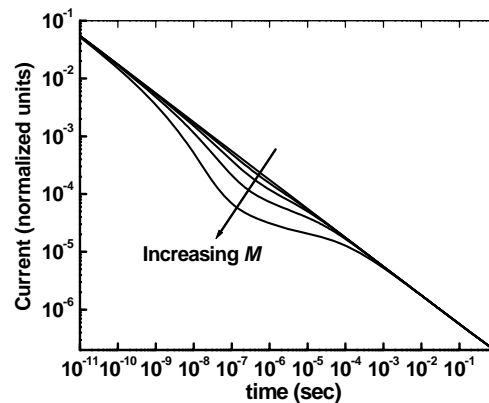
Fig. 2. Computed transient photocurrents, using the DOS of Fig. 1, normalized to the current at zero time and with no carrier losses due to arrival at an extraction electrode or to recombination. The values of M are 0, 0.3, 1, 3 and 10, increasing as indicated, and the temperature used for the simulations was 300 K.
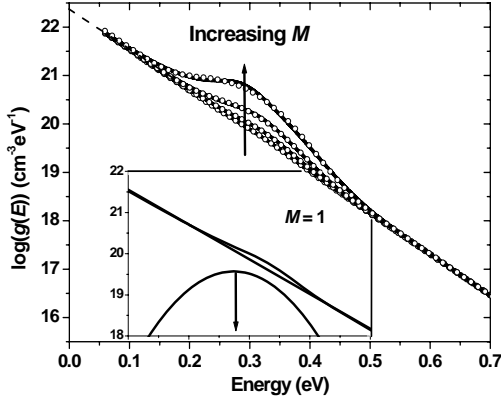
Fig 3. Density of states, as calculated using the pre-transit procedure, for the cases M = 0.3 to 10. The solid line shows the data, and the open circles are fits to an exponential bandtail plus a Gaussian feature. The inset graph indicates the individual fitted components for the case M = 1.

Fig. 3 displays the DOS values, as calculated using the pre-transit procedure, for the cases $M = 0.3$, 1, 3 and 10. It also shows iterative fits, with the parameters $g(E_c)$, T_o, $g(E_{pk})$, E_{pk} and E_w all being totally free variables. The inset shows the contributions of the various components to the computed DOS for the case $M = 1$. While the fitting procedure gives excellent agreement for $M = 3$ or less, it can be seen that the fit is not quite so precise for the case $M = 10$.

Note that with the normalized currents in Fig. 2, the conversion expression for the pre-transit procedure is reduced to $g(E) = (1/I(t).t) (g(E_c)/\nu)$, with $g(E_c) = 4 \times 10^{21}$ cm^{-3}eV^{-1} and $\nu = 10^{12}$ Hz, as employed in all of the present simulations.

Of course, although the technique of fitting data to a known functional DOS works effectively here, it is unlikely to be applicable when interpreting actual experimental data, where an assumption of the form of the DOS would be required. Its value in the present study is to assist in the evaluation of the viabilities of the pre-transit, and (below) post-transit and FT techniques, under such "idealized" circumstances.

Note also that since one or more of the parameters $I(t=0)$, $g(E_c)$ and ν in Eq. 1 would almost certainly not be known in practice, such a quantitative conversion would not be possible in the case of experimental data. However, the first two parameters only influence the absolute magnitude of the calculated $g(E)$, while inaccuracy in the assumed value of ν will also displace the energy scale uniformly, but not influence the actual forms of the curves or the resulting values of E_{pk} and E_w.

Table 1 summarizes the data arising from such fits. The calculated fitting accuracies in the values of E_{pk} are better than ± 1 meV for $M \leq 3$, even in the case of the barely-detectable deviation of the current from the pure power-law form for $M = 0.3$ (see Fig. 2). The poorer fit for $M = 10$ results in a somewhat smaller calculated value of E_{pk}, as shown in the table.

Table 1. Fitting parameters for the DOS data in Fig. 3.

M	T_0 (K)	$g(E_{pk})$ (cm^{-3}eV^{-1})	E_{pk} (eV)	E_w (eV)
0.3	590	9.6×10^{18}	0.283	0.049
1	598	3.7×10^{19}	0.274	0.052
3	596	1.3×10^{20}	0.263	0.055
10	593	6.0×10^{20}	0.246	0.061

Critically, it is clear that all values of E_{pk} are significantly smaller than the true value of 0.35 eV. Moreover, they all lie in the general vicinity of the local *minimum* of the DOS in Fig. 1 for $M = 10$ (i.e. ~ 0.28 eV). Here, we again note the finding in [2] that sufficient structure in a DOS can completely invert its form, as calculated using the pre-transit analysis. *It now seems that this situation applies to much smaller values of M than were previously anticipated!*

Although there is a *weak* trend towards the correct value of 0.35 eV as M falls, it is clear that this might (*if at all*!) only be approached when the Gaussian component is so small as to be undetectable! Indeed, contrary to prior notional expectations, the fitted value of E_{pk} remains close to 0.28 eV, *even for the case M = 0.3*!

The fitted widths of the Gaussian component, E_w, are approximately twice the correct value of 0.025 eV. Such "kT broadening" is a well known consequence of the fact that this analytical technique assumes that all carriers trapped in a state at energy E, with a release time constant $\tau = \nu^{-1}\exp(E/kT)$, are released after *exactly* this dwell time, rather than over an appropriate probability distribution of times around it.

The values of T_o for the exponential component of the DOS are close to the true value of 600 K. However, from Fig. 3, the values of $g(E_c)$ are about a factor of six larger than the true value of 4×10^{21} cm^{-3}eV^{-1}. This illustrates a further limitation of the procedure. The states at E_{th} can never be in *complete* quasi-thermal equilibrium with the extended ones, while free carriers in the latter are still being lost to deeper-lying traps. This reduces the current relative to that in Eq. 1, and thus raises (*inter alia*) the calculated values of $g(E_c)$.

In respect of the pre-transit procedure, we may thus conclude that:

(i) Although this can provide an indication of the *presence* of the Gaussian feature, it gives a significant error in the peak energy of such a feature.

(ii) Unexpectedly, at least in terms of previous notional impressions, this situation persists even when the additional height of the feature *falls below that of the background DOS.*

3. Computer simulation results for the "post-transit" case

Fig. 4 shows data corresponding to those in Fig. 2, but with a finite and short free carrier transit time. The simulation parameters were $g(E_c) = 4 \times 10^{21}$ (cm^{-3}eV^{-1}), $Q_0 = 1.6 \times 10^{-9}$ C, $t_0 = 2 \times 10^{-11}$ sec. and $\nu = 10^{12}$ Hz, giving the conversion parameter $C = 2 \ g(E_c)/(Q_0 \ t_0 \ \nu)$ in Eq. 2 as 2.5×10^{29} cm^{-3}eV^{-1}C^{-1}.
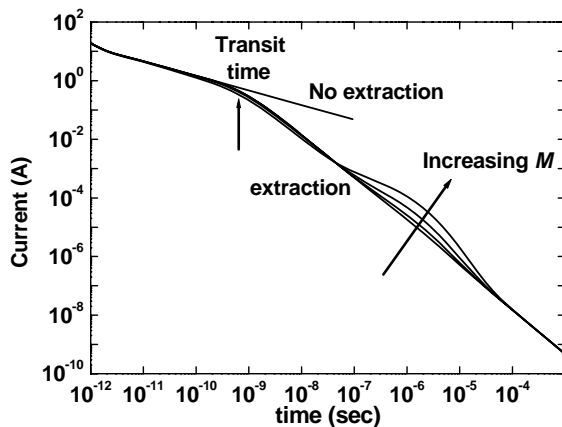
Fig 4. Computer simulated current at T = 300 K, for values of M of 0.3, 1, 3 and 10, increasing in the direction indicated. In this case, the simulation parameters (see text) were set to yield a short transit time. The graph also shows the current that would be obtained in the case of an infinitely thick specimen (i.e. with no carrier extraction).

Fig. 5 presents the resulting calculated DOS data, and Table 2 shows the associated fitting parameters. For $M \leq 3$, the values of $g(E_c)$ and T_0 are very close to the correct figures of 4×10^{21} cm^{-3}eV^{-1} and 600 K, respectively. The agreement is less precise for the case $M = 10$, where the large Gaussian component significantly influences the current at shorter times, and thus the corresponding calculated DOS.

All of the E_{pk} values are now within 1% of the correct one of 0.35 eV. The E_w values are now approximately 40% larger than the true value of 0.025 eV. This indicates a reduced degree of thermally-induced broadening, to ~ kT/2. This broadening also influences the fitted heights of the Gaussian component. The $g(E_{pk})$ value should be 4.5×10^{18} cm^{-3}eV^{-1} for the case $M = 1$, and proportionately lower or higher for the other cases. This effect is approximately what would be expected if the total area under the Gaussian component is preserved in the presence of the broadening. The whole recovered DOS – (band-tail and feature) is now lower than that obtained by the pre-

transit method, and is much closer to the original DOS. The reduced broadening of the post-transit calculated Gaussian feature accounts for its maximum being higher and hence closer to the tail in the inset to Fig. 5 than in the inset to Fig. 3.
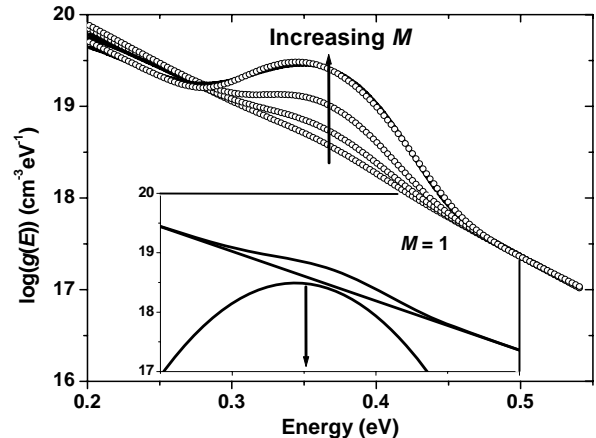
Fig. 5. Density of states, as calculated using the post-transit procedure, for the cases M = 0.3 to 10. The solid line shows the data, and the open circles are fits to an exponential bandtail plus a Gaussian feature. The inset graph indicates the individual fitted components for the case M = 1.

Table 2. Fitting parameters for the DOS data in Fig. 5.

M	T_0 (K)	$g(E_{pk})$ (cm^{-3}eV^{-1})	E_{pk} (eV)	E_w (eV)
0.3	603	9.8×10^{17}	0.342	0.036
1	607	3.1×10^{18}	0.344	0.035
3	598	8.5×10^{18}	0.349	0.033
10	642	2.7×10^{19}	0.348	0.034

Overall, and in dramatic contrast to the case of the pre-transit analysis, we conclude that the post-transit procedure is effective in revealing the DOS, irrespective (subject to quite limited thermally-induced broadening) of the degree of structure present within it.

4. Fourier transform analysis of the simulation data

Figs. 6 and 7 show the results of an analysis of the pre- and post-transit data using the Fourier transform method, and Table 3 presents the fitted parameters. It can be seen that the iterative fits are again very good, and the calculated peak energies of the Gaussian component are extremely close to the correct value of 0.35 eV. The

degree of thermal broadening is comparable to that obtained using the post-transit analysis, and is obviously a significant improvement upon that for the pre-transit case.
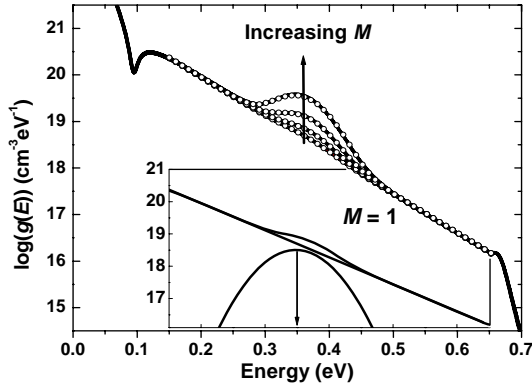
Fig. 6. Densities of states, as calculated using the Fourier transform analysis of the pre-transit data.
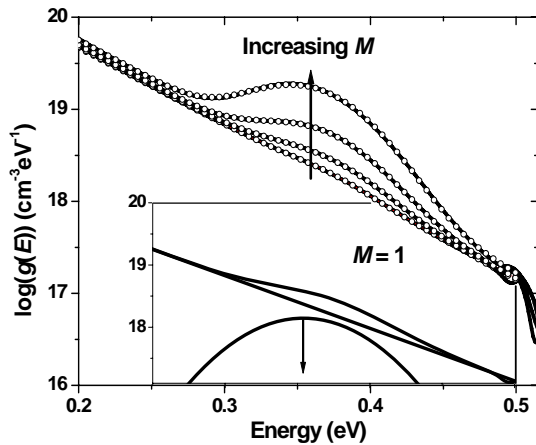
Fig. 7. The post-transit data, for the cases M = 0.3 to 10. The solid lines show the data, and the open circles are fits to an exponential bandtail plus a Gaussian feature. The inset indicates the individual fitted components for the case M = 1.

Table 3. Fitting parameters for the FT DOS data in Figs. 6 and 7.

M	T_0 (K)	$g(E_{pk})$ $(cm^{-3}eV^{-1})$	E_{pk} (eV)	E_w (eV)
Fig. 6 – pre-transit data				
0.3	604	1.0×10^{18}	0.345	0.037
1	604	3.2×10^{18}	0.348	0.036
3	604	9.4×10^{18}	0.349	0.035
10	603	3.7×10^{19}	0.350	0.035
Fig. 7 – post-transit data				
0.3	605	3.7×10^{17}	0.359	0.030
1	598	1.4×10^{18}	0.354	0.036
3	597	4.3×10^{18}	0.353	0.036
10	597	1.5×10^{19}	0.351	0.036

The distortions of the calculated DOS at the extremes of the energy ranges are due to the truncation of information about the current at very short and very long times. We have recently found that improved apodization techniques can significantly reduce this effect (see section 6). It will also be noted that the values of $g(E_c)$ and $g(E_{pk})$ for the post-transit data are about 50% of those expected. This is due to subtle differences between the effects of carrier losses by recombination (as assumed in the Fourier transform procedure) and by arrival at an extraction electrode (as in the present simulations).

5. The Potential value of measurements at different temperatures

We now turn to the effect of the measurement temperature upon the data extracted using the three techniques. The thermalization energy concept gives a time corresponding to the peak energy of $t_{th} = v^{-1}\exp(E_{th}/kT)$, which can be re-written as $\ln(t_{th}) = \ln(v^{-1}) + E_{th}(1/kT)$. Thus, in our case, a plot of $\ln(t_{pk})$ vs $(1/kT)$ should have a gradient of E_{pk}, and an intercept of $\ln(v^{-1})$. The potential value of such a plot is to eliminate the need to *assume* a value of v in determining the DOS, thereby not only giving an improved value for the peak energy of any feature under examination, but also offering an indication of the *nature* of the localized states, since their capture cross section, σ, and thus charged or neutral (when empty) state can be inferred from v, via detailed balance considerations, i.e.,
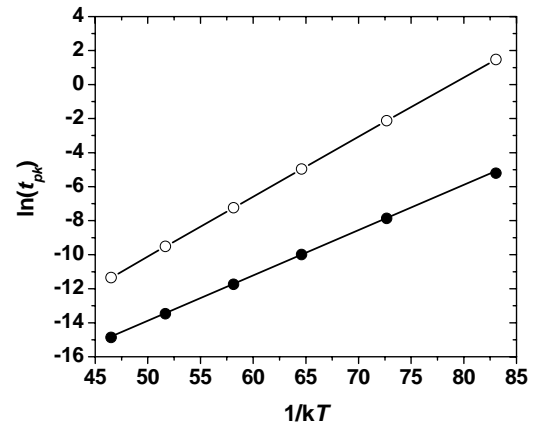
Fig. 8. Inverse temperature dependence of the time t_{pk} corresponding to E_{pk}, as determined using the pre-transit (filled circles) and FT techniques (open circles), for simulation data generated with no carrier losses by completion of transit or recombination.

$$\sigma = v / (g(E_c)kTv_{th}), \qquad (6)$$

where v_{th} is the thermal velocity of the charge carriers (weakly temperature dependent but expected to be ~ 10^7 cm.sec^{-1} at normal temperatures).

We have thus examined the temperature dependence of the time corresponding to the value of E_{pk} for the case $M = 1$, for the case of no carrier losses by arrival at an extraction electrode or recombination. The results are shown in Fig. 8. For the pre-transit analysis, the intercept is -27.15, yielding $\nu = 6.2 \times 10^{11}$ Hz, which is acceptably close to the true value of 1×10^{12} Hz However, the gradient yields $E_{pk} = 0.265 \pm 0.002$ eV, which is similar to the values in Table 1. This is obviously again incompatible with the true value of 0.35 eV and is also close to the energy of the local minimum (at ~ 0.28 eV) in the DOS for larger values of M. For the FT analysis, the corresponding values are $E_{pk} = 0.351$ eV and $\nu = 1.03 \times 10^{12}$ Hz. The results of a similar analysis of simulation data with a very short transit time, as interpreted using both the post-transit and the FT procedure, yield similar close agreement.

We have also examined a limited number other cases (specifically T_0 values of 400 and 800 K with other parameters as above), and have established that the inaccuracies arising from the pre-transit analytical procedure are similar to those presented above, in terms of the resulting values of E_{pk} etc. Thus, we can state that even though this problem may not be *totally* universal, the potential error in the energy placement of any significant feature in the DOS is sufficient in itself to invalidate any *confident* use of the procedure.

6. Discussion of the Fourier transform method

We present a short explanatory note here on the practical application of the Fourier Transform method – treating in particular, the approach used to minimise errors arising from limited instrumental rise-time and truncation of time-sampled data at both short and long times.

The rationale for making the conversion to the frequency domain has been alluded to in section 1. In essence, in all of the above, we are seeking to extract, from the measured $i(t)$ data, information on the distribution of trapping times and associated release times for each part of the trap distribution. In this context, the direct use of time-domain data is fraught with difficulty, since during the photocurrent decay, the traps act in concert and their effects on the free carrier density are not independent. The information we seek is thus encoded as a *convolution* of all of the trap system responses and is additionally convolved with the instrument system response. The instantaneous $i(t)$ cannot, except under severely restricted conditions 'disentangle' the trapping and release time information.

However, in the frequency domain, $I(\omega)$, including phase information $\phi(\omega)$, contains the required information in un-encoded form, as simple products and sums, which are easily analysed. Nevertheless, for accurate application of the one sided Fourier Transform, we require data in the range $0 \le t \le \infty$. In practice, as for all DFT situations, the experimental time range available for the DFT summation

typified in Eq. 3 is necessarily restricted, and moreover, at short times, the instrument time response will distort the short-time $i(t)$ data. Fig. 9 shows simulated $i(t)$ data illustrating these points. For this illustration, we have used a system response with a single dominant pole at 10^{-9}s, and a sampled-time range of $10^{-9} s \le t \le 1s$. We note that higher order response functions could in principle be treated in the same way. Truncation of the time domain data at short and long times produces effectively, via the DFT, the convolution of the (already distorted) data with a rectangular function, as shown.
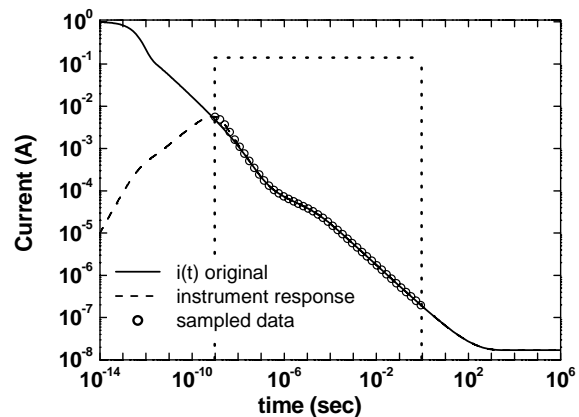
Fig. 9. Simulated i(t) for the M = 3 case, with the effects of instrumental time response and sampled-data time-truncation indicated.

The abrupt truncation of $i(t)$ at long times will, on application of the DFT, generate a distribution of high order harmonics which will be manifested as substantial errors in the calculated DOS at deep energies, and spread over a wide energy range. In addition to the instrumental rise-time distortion at short times, the short-time truncation of $i(t)$ has the effect of removing the initial part of the Fourier integral, which can result in large errors in the calculated DOS at shallow energies. We address both of these problems below.

For the long-time truncation problem, standard digital signal processing (DSP) practice employs apodization procedures which use window functions to 'taper off' the data to minimise the generation of higher order harmonics in the DFT. Various such window functions (Gaussian, Blackmann, Hann, Kaiser [11]) were applied to the present data, to good effect.

Fig. 10 demonstrates the effect of apodization. Here we compare the DOS computed using Eq. 4, for three time-domain $i(t)$ data sets based again on the M=3 case. For DOS (a), we have used a very wide time range $10^{-16} s \le t \le 10^{10} s$ to approach the 'true' FT of the $i(t)$ data, while (b) uses the abruptly truncated data of Fig. 9. For the third computed DOS, (c), we have imposed a

Kaiser Bessel window function with parameter $\alpha = 2$, on the truncated data of Fig. 9. Note that this last plot has also been 'short-time-corrected' by a procedure which will be described below.
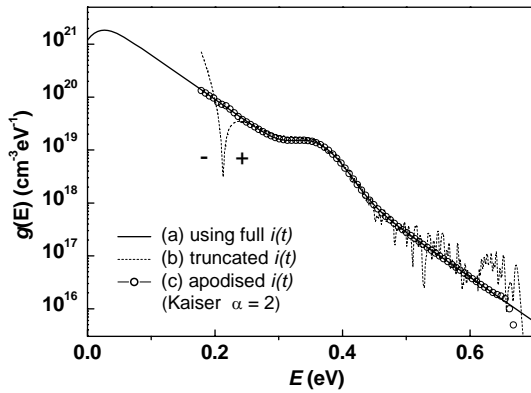
Fig. 10. DOS calculated by FT from i(t) for the M= 3 case, using; (a) i(t) data for $10^{-16} s \leq t \leq 10^{10} s$; (b) sampled and time-truncated data as shown in fig. 9; (c) the same data with long-time apodization using a Kaiser Bessel window. Note that (c) additionally uses i(t) correction at short times, as outlined in the text .

It can be seen that using a very wide time-range of $i(t)$ allows an accurate reconstruction of the 'starting' DOS over a wide range of energies, to within about kT of the band edge. On the other hand, using the truncated $i(t)$ data with no apodization, leads to 'apparently unsystematic', sharply varying errors of up to an order of magnitude, over a surprisingly wide energy range, from 0.7 eV depth up to 0.4 eV from the band edge. At the top of the DOS plot, the short-time truncation has produced a large systematic error in the shallow DOS, even producing a sign change at energies less than ~ 0.2 eV!

On application of apodization, the long-time errors are substantially removed, and only the 'bottom $2kT$' of the available deep trap energy range is lost.

We next attempt to take account of the inaccessible short time $i(t)$ in a simple two step procedure. The first step, made in the *time domain*, extrapolates the response backwards toward $t = 0$, whilst retaining the effects of instrumental rise time. The second step makes a correction for the instrument response, but in the *frequency domain*.

The time domain extrapolation is an iterative procedure using the known value of the system dominant pole, the measured initial photocurrent $i(t_1)$ and average initial measured slope, di/dt. Assuming the short time current is of the general form

$$i(t) = \frac{2i_0}{1 + (t/t_0)^x}, \qquad (7)$$

it is possible to use this to solve numerically (for x) for the resulting instrumentally modified time response so as to 'patch' the constructed current on to the initial sampled

data with the appropriate slope. Typically, a value of $t_0 \sim 1/v$ has been used, but it turns out that the procedure is not too sensitive to variation in this value. Note that the value of i_0 is just a formal result of the procedure, and may not equal the actual initial current at $t = 0$.
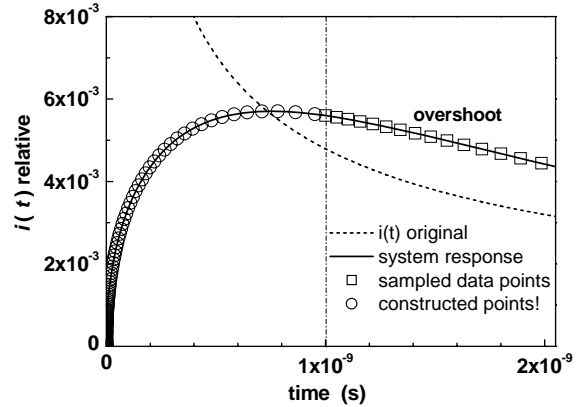
Fig. 11. Linear plot showing how i(t) - modified by the system response at short times may be constructed by extrapolation of longer time sampled data.

It may be argued that this procedure is limited in that it presumes a power law form of decay. We note that the variation allowed in index x has produced reasonably good fits to data in which the original $i(t)$ falls between such extremes as 'flat', and an exponential decay. In addition, normally we need only aim for a reasonable fit in the restricted range $t_1/10 \leq t \leq t_1$, which relaxes the fitting conditions somewhat.

Fig. 11 illustrates this procedure, applied to the simulation data of Fig. 9 for the case M=3. Here we have a system rise time of 1ns, and a first sample point also at $t = 1$ns, although the procedure allows these times to differ from each other by at least an order of magnitude.
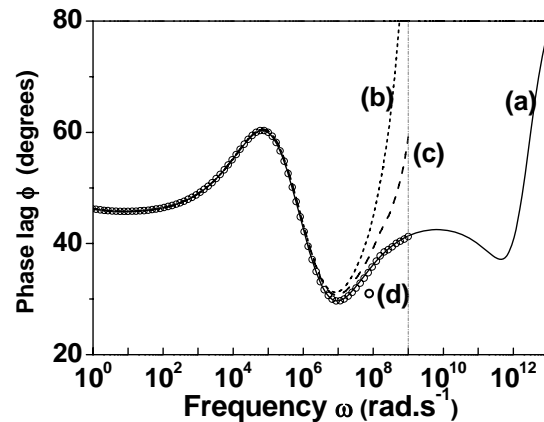
Fig. 12. Phase shift $\phi(\omega)$ computed via DFT for the simulated i(t) under several conditions. (a) Full i(t) curve, (b) truncated i(t) after instrumental response, with

no time domain or frequency domain correction, (c) truncated i(t) after instrumental response, with only time domain correction, (d) truncated i(t) after instrumental response, with time and frequency domain corrections.

It is evident from Fig. 11 that the system response can have a significant distorting effect on the *i(t)* curve. The resulting response starts from zero, and often, as here, exhibits a large overshoot above the actual *i(t)* response, not approaching the true response until as much as one order of magnitude in time beyond the system rise-time. In the past, this portion of the recorded data was often discarded. Here, we recognize that useful information is embedded in this part of the response, and may be extracted, given knowledge of the system response. We have reported on earlier approaches to this topic in several publications [12,13]

Application of the first step of the procedure described above, using the first sampled data point at t = 1ns, and the slope between this point and t = 2ns, results in the constructed curve (symbol ○) for t < 1ns. It is clear that in this case, the fit to the instrumentally modified short time response is very good.

A DFT performed on the composite *i(t)* data will be much more accurate, at least up to a frequency $\omega_1 \sim 1/t_1$, than a DFT taken without the short-time construction, thus extending the reliable upper energy range of the method to $E_1 = kT \ln(\nu/\omega_1)$. However, the second correction step, in the frequency domain, must also be completed.

The frequency domain correction is straightforward. Knowing the instrumental system transfer function $\widetilde{H}(\omega) = \left|\widetilde{H}(\omega)\right| \angle\theta(\omega)$, which is in this case a simple single pole response, we can apply multiplicative and additive corrections to the DFT amplitude and phase respectively. Other transfer functions, if known, can be treated equally easily at this point.

In Fig. 12, we show the effect of both the time and frequency domain corrections on the computed DFT phase shift $\phi(\omega)$.In this case, a substantial improvement is evident, which results in a great reduction in error in the DOS computation for shallow energies, as illustrated in Fig. 10.

7. Conclusions

We have demonstrated that even for the case of a *very* small deviation from an exponential DOS, as induced by the addition of a narrow Gaussian component, application of the pre-transit $(1/I(t).t)$ analytical technique yields a significant error in respect of the peak energy of this feature.

If our results can be generalized to other forms of DOS, and we see no reason why this should not be the case, then this technique (despite its attractive simplicity) appears inapplicable in respect of *any* attempted quantitative study of localized state distributions in disordered semiconductor materials.

In contrast, we have also demonstrated that both the post-transit and Fourier transform techniques can yield accurate representations of the DOS, and therefore remain valid.

Recent improvements in the Fourier Transform method procedures have also been outlined, dealing in particular with the minimisation of short- and long-time data truncation effects. Substantial improvements are shown to be achievable.

References

[1] J. M. Marshall, R. A. Street, Solid State Commun. **50**, 91 (1984).
[2] J. M. Marshall, C. Main, Phil. Mag. B **47**, 471 (1983).
[3] J. M. Marshall, Reports on Progress in Physics **46**, 1235 (1983).
[4] T. Tiedje, A. Rose, Solid State Commun. **37**, 49 (1980).
[5] G. F. Seynhaeve, R. P. Barclay, G. J. Adriaenssens, J. M. Marshall, Phys. Rev. B **39**, 10196 (1989).
[6] C. Main, R. Brüggemann, D. P. Webb, S. Reynolds, Solid State Commun. **93**, 401 (1992).
[7] C. Main, Mat. Res. Soc. Symp. Proc. **467**, 167 (1997).
[8] C. Main, J. Non-Cryst Solids **299-302**, 525 (2002)
[9] K. Hattori, Y. Niwano, H. Okamoto, Y. Hamakawa, J. Non-Cryst. Solids **137 & 138**, 363 (1991).
[10] C. Main, J. Berkin, A. Merazga, in New Physical Problems in Electronic Materials, ed. M. Borissov, N. Kirov, J. M. Marshall and A. Vavrek (World Scientific, Singapore, 1991) p. 55.
[11] F. J. Harris, Proc. IEEE **66**, 51–83 (1978).
[12] S. Reynolds, C. Main, D. P. Webb, S. Grabtchak, J. Appl. Phys. **88**, 278 (2000).
[13] C. Longeaud, C. Main, J. Phys.: Condens. Matter **20**, 135217 (2008).

_____
[*]Corresponding author: c.main@dundee.ac.uk